

See discussions, stats, and author profiles for this publication at: <https://www.researchgate.net/publication/268878689>

The Relationship between Oxygen Permeability and Phase Separation Morphology of the Multicomponent Silicone Hydrogels

ARTICLE *in* THE JOURNAL OF PHYSICAL CHEMISTRY B · NOVEMBER 2014

Impact Factor: 3.3 · DOI: 10.1021/jp507682k · Source: PubMed

CITATIONS

3

READS

53

4 AUTHORS, INCLUDING:



Yong Jiang

Southeast University (China)

49 PUBLICATIONS 938 CITATIONS

SEE PROFILE

The Relationship between Oxygen Permeability and Phase Separation Morphology of the Multicomponent Silicone Hydrogels

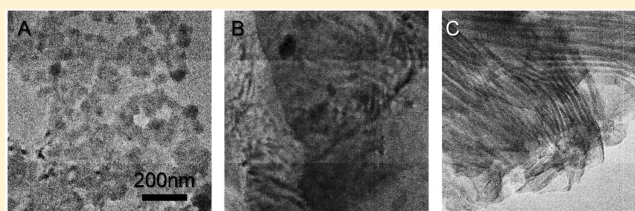
Zhengbai Zhao, Haijiao Xie, Shuangshuang An, and Yong Jiang*

School of Chemistry and Chemical Engineering, Southeast University, Jiangning, Nanjing, Jiangsu 211189, P. R. China

S Supporting Information

ABSTRACT: In this article, the multicomponent copolymers were prepared by the copolymerization of two hydrophobic silicon-containing monomers bis(trimethylsilyloxy) methylsilylpropyl glycerol methacrylate (SiMA) and tris(trimethylsilyloxy)-3-methacryloxypropylsilane (TRIS) with three hydrophilic monomers 2-hydroxyethyl methacrylate, *N*-vinylpyrrolidone, and *N,N*-dimethyl acrylamide. The copolymers were hydrated to form transparent silicone hydrogels.

The oxygen permeability coefficients (*Dk*) of hydrogels were measured, and their relationships with the equilibrium water contents (EWC) and the types and contents of silicon containing monomers as well as the phase separation structures of silicone hydrogels were analyzed in detail. The results showed that the EWC decreased as the increase of SiMA content. The relationship between *Dk* and SiMA content, as well as that between *Dk* and EWC, showed inverted bell curve distributions, which meant two main factors, i.e., silicon–oxygen bond in silicone and water in hydrogel, contributed to oxygen permeation and followed a mutual inhibition competition mechanism. The internal morphologies of the hydrogels were observed by transmission electron microscope, and the results showed that the hydrogels presented two different phase separation structures depending on the types of the silicon-containing monomers. The silicone phase in SiMA containing hydrogel presented to be a granular texture, while the silicone phase in TRIS containing hydrogel formed a fibrous texture which resulted in a higher *Dk* value. These results could help to design a silicone hydrogel with better properties and wider application.



■ INTRODUCTION

Over the last several decades, the application of hydrogel has shown steady growth, particularly in the areas of medicine, biology, materials science, and engineering.^{1–5} Specific applications of hydrogels include contact lenses,⁶ blood-contacting medical devices,⁷ drug delivery,⁸ and artificial tissue like bone or tendon or even arteries.^{9–11} These applications are owing to the impressive properties of this type of biomaterials, such as biocompatibility, mechanical strength, optical properties, gas permeability,¹² etc. Among these properties, gas permeability is one of the most important indexes that determines the wearing comfort and time of biomaterials such as contact lenses.

Previous studies have shown that phase separation morphology should be taken into consideration for gas permeation through multicomponent polymer membranes.^{13–22} The relationship between gas permeation and phase separation morphology has been studied on the basis of a variety of models^{13–15} and simulations.^{23,24} These results indicated that, owing to their unique phase separation structure, these materials have possessed a lot of excellent properties^{19–21} and attracted extensive interest because of their potential applications for binder resins, coatings, fibers, and particularly biomaterials.^{25–29} However, it is still unclear how the oxygen permeability was affected by the internal structures of different phases or the phase separation morphology. Also, the molecular mechanism of oxygen permeability is not yet settled.

Conventional hydrogels^{30,31} have good hydrophilicity but limited oxygen permeability. One known way to solve this problem is to add the high oxygen permeable silicon-containing monomers^{32–34} because silicon–oxygen bonds have a good ability for gas transmission. The oxygen permeability of silicone hydrogels has been widely investigated in the last two decades. Lai et al. prepared polysiloxane-based polyurethane and found that the oxygen permeability of the hydrogels is much higher than those of nonsilicone hydrogels and decreased as the equilibrium water content (EWC) increased.³⁵ Liu et al. synthesized a PDMS/PNIPAAm interpenetrating polymer network (IPN) that had high oxygen and glucose permeability.³⁶ Willis et al. studied a phosphorylcholine coated silicone hydrogel and discovered that the oxygen permeability of the material could be controlled by the hydrophilic:hydrophobic monomer balance in the formulation.¹² Maldonado-Codina investigated the short-term physiologic response to three soft lens materials with different permeability characteristics and suggested that silicone hydrogel could provide more oxygen to the ocular surface than conventional hydrogel.³⁷ Wang et al. prepared an IPN of silicone hydrogels with improved oxygen permeability and mechanical strength.³⁸ Pozuelo et al. discussed the transportation of oxygen, water,

Received: July 30, 2014

Revised: November 25, 2014

Published: November 25, 2014

Table 1. Copolymerization Formulations for the Multicomponent Hydrogels with Different Contents of SiMA Monomer

hydrogel	SiMA (wt %)	HEMA (wt %)	NVP (wt %)	DMA (wt %)	Dk (10^{-11} cm ² /s)	EWC (wt %)
0	0	59.5 ± 0.1	25.5 ± 0.1	15.0 ± 0.1	22.3 ± 1.7	67.8 ± 1.5
I	10.0 ± 0.1	52.5 ± 0.1	22.5 ± 0.1	15.0 ± 0.1	18.7 ± 1.4	55.7 ± 1.7
II	20.0 ± 0.1	45.5 ± 0.1	19.5 ± 0.1	15.0 ± 0.1	17.0 ± 1.5	47.6 ± 1.8
III	30.0 ± 0.1	38.5 ± 0.1	16.5 ± 0.1	15.0 ± 0.1	17.8 ± 1.2	40.1 ± 1.6
IV	40.0 ± 0.1	31.5 ± 0.1	13.5 ± 0.1	15.0 ± 0.1	19.3 ± 1.6	34.5 ± 1.8
V	50.0 ± 0.1	24.5 ± 0.1	10.5 ± 0.1	15.0 ± 0.1	34.5 ± 3.4	30.0 ± 1.7

and naked ions in two hydrogel materials; one was a conventional hydrogel based on hydroxyethyl methacrylate, and the other was a silicone hydrogel material containing siloxane moieties.³⁹ However, the main focus of this research was to develop new silicone hydrogel materials with good oxygen permeability for application purposes. Little concern was focused on the fundamental relationship between the mechanism of oxygen permeability and the internal morphology of different phases.

We have done a great deal of work on the cross-linked copolymerization of multicomponent monomers with different properties to prepare multifunctional hydrogel.⁴⁰ A series of multicomponent hydrogels were prepared by the copolymerization of several silicon-containing monomers with the different hydrophilic monomers. During the preparation, the properties of the obtained copolymers/hydrogels were studied in detail. The ethanol extraction experiments as well as the FT-IR, DSC, and TG results showed that copolymerization was effective. The optical, permeability, and mechanical analysis results demonstrated that the obtained hydrogel was highly transparent with good oxygen permeability and mechanical properties, and the impact of cross-linker on the mechanical properties of the hydrogel was also discussed in detail.

In this work, several series of experiments were designed in order to study the relationship between the oxygen permeability and microphase separation structure. The oxygen permeability coefficient (Dk) and the phase separation texture were explored by polarography and transmission electron microscope (TEM), respectively. Also, the relationships between the oxygen permeability and EWC as well as the content of silicon-containing monomer and the internal morphology of hydrogel were discussed. On the basis of this study, the relationship between oxygen permeability and phase separation morphology was established and the mechanism of oxygen permeation was proposed.

EXPERIMENTAL SECTION

Materials. Bis(trimethylsilyloxy) methylsilylpropyl glycerol methacrylate (SiMA, CAS No.: 69861-02-5) was purchased from Cornelius Specification Ltd. Tris(trimethylsiloxy)-3-methacryloxypropyl-silane (TRIS, CAS No.: 17096-07-0) was purchased from Alfa Aesar Chemical Co. 2-Hydroxyethyl methacrylate (HEMA) was obtained from BASF Chemical Co. *N,N*-Dimethyl acrylamide (DMA) was bought from Aldrich Chemical Co. *N*-Vinylpyrrolidone (NVP), methyl acrylic acid (MAA), ethylene glycol dimethacrylate (EGDMA), and 2-hydroxy-2-methylbenzene acetone (D-1173) were purchased from TCI Development (Shanghai). Ethanol and hexanol were purchased from Sino Pharm Chemical Reagent Co. Phosphate buffered saline (0.1 M, pH 7.2) was prepared by our own laboratory.

Methods for Preparing Silicone Hydrogel. For making multicomponent hydrogels, the photo initiator D-1173 and the

cross-linking agent EGDMA were added in the beaker first. Then, HEMA, NVP, TRIS, and SiMA were added in that order. After that, a certain amount of DMA was added into the mixture. At last, the solvent hexanol was added. The formulation mixture was stirred for 2 h in the dark at room temperature (25 °C). Then, the mixture was transferred to double stack polypropylene molds and UV (≥ 15 mV/cm²) initiated for the copolymerization for 3 h at room temperature. The newly formed copolymer was purified by extraction with ethanol for 16 hours and then hydrated in boiling water for 4 h. The obtained hydrogels were preserved in phosphate buffered saline. A series of silicone hydrogels were prepared using the formula list in Table 1. For all the formulations, the amounts of the cross-linking agent EGDMA and the initiator D-1173 used were 1 and 0.2 wt %, respectively.⁴⁰

Measurement of Equilibrium Water Content (EWC).

The obtained film was dried using a vacuum oven at a temperature of 90 °C, and the dry weight G_1 was accurately measured. Then, the dried film was hydrated in boiling water for 4 h. The film was placed between two pieces of filter paper to absorb the water on the surface. Finally, the wet weight G_2 was measured. EWC (η) was calculated by the following equation: $\eta = [(G_2 - G_1)/G_1] \times 100\%$.

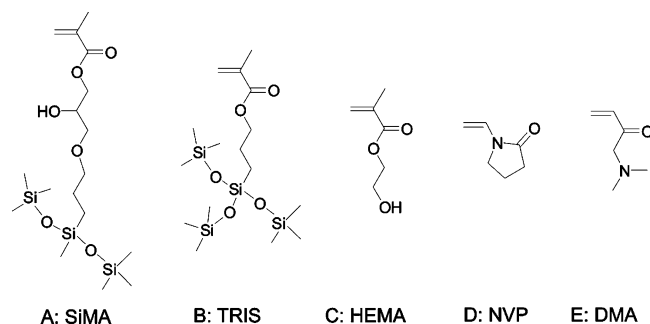
Measurement of Oxygen Permeability Coefficient (Dk). The Dk value of the silicone hydrogel was measured by using an oxygen permeation analyzer (Createch 201T Oxygen Permeameter) via AC polarography. After being fully hydrated in PBS solution (pH 7.2), the hydrogels were measured to get their center thickness. Then, these samples were put on the electrode successively and polarography was used to measure the electric current values. The temperature should be controlled at 35 ± 5 °C. The air humidity should be controlled at about 95%. Finally, we calculated the slope of the center thickness–electric current value curve to get the Dk value. The measured values of oxygen permeability were expressed in terms of barrier, which represented the volume of oxygen transmitted (10^{-11} cm²/s).

Measurement of Internal Morphology. The internal morphology of the dried silicone hydrogel was characterized by TEM (JEM-2100), and the elemental composition of different areas in silicone hydrogels was characterized using SEM/EDS (FEI Inspect F50). The hydrogels were cooled down using liquid nitrogen and then ground rapidly into powder and dispersed in water again. These mixtures were stored in tubes and incubated overnight. For preparing TEM samples, we first shook these tubes and then took the mixtures out using a pipet to add them to copper grids. Then, the samples were dried using an infrared lamp. These samples were characterized by TEM at an operating voltage of 200 kV in a vacuum. For preparing SEM samples, we poured the water out of the tubes and dried the samples by using a vacuum drying oven at 90 °C for 12 h. Then, we glued the powder to the conductive tapes.

RESULTS AND DISCUSSION

In order to test how the silicon-containing monomer affects the EWC and oxygen permeability of hydrogel, two different kinds of silicon-containing monomers were chosen to prepare silicone hydrogels. One is SiMA in Scheme 1A, which has

Scheme 1. Chemical Structures of the Monomers Used for Preparing Multicomponent Hydrogels^a



^a(A) Bis(trimethylsilyloxy) methylsilylpropyl glycerol methacrylate (SiMA), (B) tris(trimethylsilyloxy)-3-methacryloxypropylsilane (TRIS), (C) 2-hydroxyethyl methacrylate (HEMA), (D) *N*-vinyl pyrrolidone (NVP), and (E) *N,N*-dimethyl acrylamide (DMA).

three silicon atoms in each monomer, and the other is TRIS (Scheme 1B), which has four silicon atoms in the monomer. Since the silicon-containing monomers are relatively hydrophobic, in order to make the hydrogel more hydrophilic, as well as increase the mechanical properties of the hydrogel, three hydrophilic monomers were copolymerized into the hydrogels together to form multicomponent networks. Scheme 1 lists all the monomers that we used in this paper.

In order to test the influence of the content of silicon-containing monomer on the EWC and oxygen permeability, a series of silicone hydrogels were copolymerized with different contents of SiMA monomer. The formulations are listed in Table 1, where the percentages of SiMA increased from 0 to 50 wt %, while the percentages of HEMA and NVP decreased correspondingly. In this formulation, the ratios of HEMA and NVP for different hydrogels were fixed at 7:3 and the percentage of DMA was fixed at 15 wt %. After the copolymers were prepared, the ethanol extraction experiments as well as the FT-IR, DSC, and TG were carried out to study the copolymerization and the results showed that copolymerization was effective.⁴⁰

Figure 1A shows the relationship between the EWC of silicone hydrogel and the content of SiMA monomer. The EWC of silicone hydrogels decreased along with the increase of SiMA. The EWC was 67.8 ± 1.5 wt % without adding SiMA, and the value decreased to 30.0 ± 1.7 wt % when the content of SiMA was increased to 50 wt %. It is clear that HEMA, NVP, and DMA are hydrophilic monomers, while SiMA is relatively hydrophobic even though it has a hydroxyl group on its side chain; therefore, it is understandable that adding SiMA resulted in a decrease of the EWC of the hydrogels.

Figure 1B shows the relationship between Dk and the SiMA content in multicomponent hydrogels. As shown in Figure 1B, at the point of zero on the horizontal axis where no SiMA was included, the Dk value of the hydrogel was about 22.3 ± 1.7 . Along with the increase of SiMA content from 0 to 20 wt %, the Dk value dropped slowly and reached the minimum value of 17.0 ± 1.5 at the SiMA content of 20 wt %. After that, the Dk values began to rise with the increase of SiMA content. When the SiMA content exceeded 40 wt %, the Dk value increased dramatically and reached 34.5 ± 3.4 at a SiMA content of 50 wt %.

TEM was used to observe the internal morphology of these hydrogels in order to further explain the oxygen transmission mechanism from its delicate structure. Figure 2 shows the

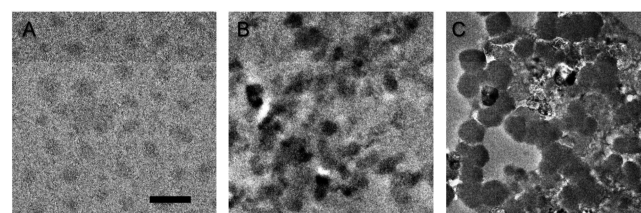


Figure 2. TEM graphs of silicone hydrogels with the SiMA content of (A) 10 wt %, (B) 20 wt %, and (C) 50 wt %, respectively. Scale bar = 200 nm.

morphology of the silicone hydrogel with different SiMA content. It could be clearly seen that the silicone hydrogels showed a phase separation structure where the silicone phase had a granular texture. The silicone phase in the images presented to be darker grains because silicon is the biggest atom and has the highest electronic contrast in the multicomponent hydrogel. When 10 wt % SiMA was added, as shown in Figure 2A, the silicone phase was discontinuous and presented to be gray grains with a size less than 100 nm, while the continuous phase was hydrogel formed by hydrophilic

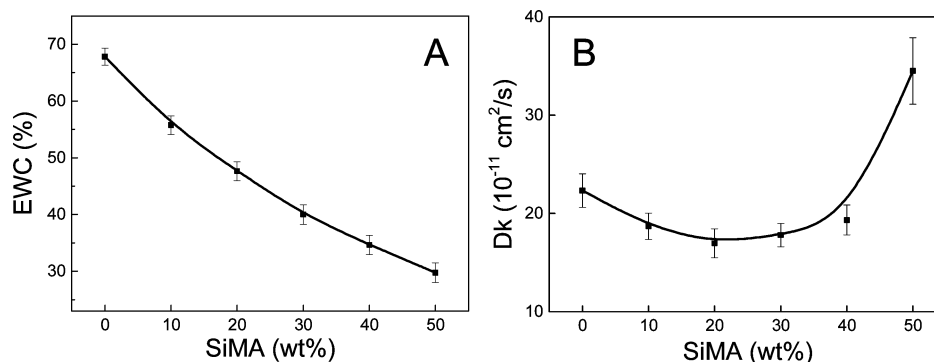


Figure 1. (A) The percentage of EWC and (B) the value of oxygen permeability coefficient (Dk) as functions of the SiMA percentage in the multicomponent hydrogels.

Table 2. Copolymerization Formulations for the Multicomponent Hydrogels with Different Contents of MAA Monomer

hydrogel	SiMA (wt %)	HEMA (wt %)	NVP (wt %)	DMA (wt %)	MAA (wt %)	Dk (10^{-11} cm ² /s)	EWc (wt %)
V	50.0 ± 0.1	24.5 ± 0.1	10.5 ± 0.1	15.0 ± 0.1	0	34.5 ± 3.4	30.0 ± 1.7
VI	50.0 ± 0.1	23.1 ± 0.1	9.9 ± 0.1	15.0 ± 0.1	2 ± 0.1	23.4 ± 1.4	43.0 ± 1.2
VII	50.0 ± 0.1	21.0 ± 0.1	9.0 ± 0.1	15.0 ± 0.1	5 ± 0.1	26.6 ± 1.1	48.1 ± 1.0
VIII	50.0 ± 0.1	17.5 ± 0.1	7.5 ± 0.1	15.0 ± 0.1	10 ± 0.1	37.2 ± 1.8	56.5 ± 1.4

monomers. When 20 wt % SiMA was added, as shown in Figure 2B, the silicone grains became darker and denser and part of them began to gather together to form continuous phase. When the SiMA content reached 50 wt % (Figure 2C), the silicone phase became deep black grains and the size increased to about 130 nm, which resulted in the silicone phases contacted with each other to form a continuous phase, and at the same time, the hydrogel phase was separated and became discontinuous.

In silicone hydrogel with phase separation structure, oxygen permeation is contributed by both the silicone phase and the hydrogel phase together. Before the silicone phase became continuous, oxygen permeation was mainly through the water in the hydrogel phase. The discontinuous silicone phase could not contribute to oxygen transportation but led to the decrease of the percentage of EWC in the silicone hydrogel and then blocked the oxygen diffusion. As a result, the Dk decreased when the SiMA content increased at this stage. However, when the percentage of SiMA content was higher than 20 wt %, the silicone phase became continuous and contributed to the oxygen permeation. At this time, the silicone phase turned into the main channel for oxygen transportation. As a result, the Dk increased dramatically because the silicon–oxygen bond in the silicone phase has a better oxygen permeability than the water in the hydrogel phase. Thus, in this study, the silicone hydrogel with 20 wt % SiMA was the critical point for the phase inversion to take place, where the Dk reached the lowest point.

The surface morphologies and chemical compositions of the cross sections of silicone hydrogel with different SiMA contents were observed and analyzed by scanning electron microscope and energy-dispersive X-ray spectroscopy. The results were shown in Figure S1 and Table S1 (Supporting Information). To perform this measurement, silicone hydrogels were grounded into powder in order to observe internal structures. The results showed that the internal compositions were not homogeneous. Thus, the images and tables can be used as secondary proof to verify that the microphase separation structure exists in the internal hydrogel.

In order to test our theory that both the silicone phase and the hydrogel phase contradicted with each other in terms of the contribution to oxygen permeability, another series of silicone hydrogel were prepared, in which the content of SiMA was fixed and the EWC increased gradually. For this purpose, MAA was added into the formulation in order to adjust the EWC. The formulations are shown in Table 2, where the SiMA content was fixed at 50 wt %, while the contents of HEMA and NVP decreased according to the increasing content of MAA.

As shown in Figure 3, the Dk value did not always increase with the increase of EWC. However, the influence of the percentage of EWC to the oxygen permeability was similar to that of the SiMA content. The Dk value decreased from 34.5 ± 3.4 to 23.4 ± 1.4 when the percentage of EWC increased from 30.0 ± 1.7 to 43.0 ± 1.2 wt %. However, the Dk value began to increase when the EWC increased further. The Dk was 37.2 ± 1.8 when the EWC was 56.5 ± 1.4 wt %.

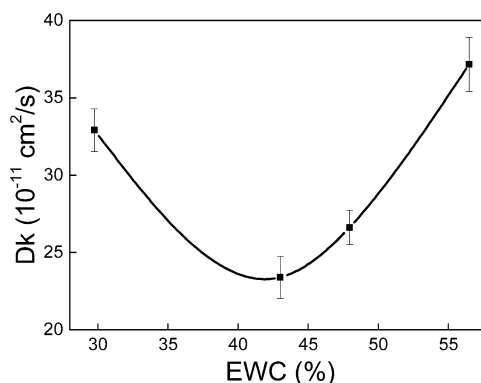


Figure 3. Value of Dk as a function of the percentage of EWC in silicone hydrogels. The SiMA contents in these hydrogels were fixed at 50 wt % and the contents of HEMA, NVP, and DMA decreased accordingly as the increasing content of MAA.

When the EWC was less than 43.0 wt %, hydrogel was a discontinuous phase. At this stage, increasing the EWC would not contribute to the oxygen permeation but destroyed the silicone phase, and as a result of it, the Dk decreased. However, when the EWC was higher than 43.0 wt %, the hydrogel phase became continuous and would mainly contribute to the oxygen permeation. As a result of it, the Dk increased. Thus, for this series of silicone hydrogel, 43.0 wt % EWC was the critical percentage for the phase inversion to take place, where Dk reached the lowest point.

On the basis of the above research, the influences of the percentages of EWC and SiMA on oxygen permeation were well-established. To verify the ubiquity of the mechanism, another silicon-containing monomer TRIS was selected, whose chemical structure is shown in Scheme 1B. These two monomers have very close molecular weights (SiMA, 422.7; TRIS, 422.8), while TRIS possesses one more silicon-containing group than SiMA. One series of silicone hydrogels was copolymerized using different contents of TRIS monomer to replace SiMA. The formulations were listed in Table S2 (Supporting Information), where the percentages of TRIS increased from 0 to 30 wt %, while the percentages of HEMA and NVP decreased correspondingly. In these formulations, the ratios of HEMA and NVP for different hydrogels and the percentage of DMA were the same as the values shown in Table 1. Another series of silicone hydrogels was prepared, in which the content of TRIS was constant and the EWC increased gradually. The formulations were shown in Table S3 (Supporting Information), where the TRIS content was fixed at 30 wt %, while the contents of HEMA and NVP decreased according to the increasing content of MAA.

Figure S2A (Supporting Information) shows the relationship between Dk and the TRIS content in the multicomponent hydrogel. At the point of zero on the horizontal axis where no TRIS was included, the Dk value of hydrogel was about 22.4 ± 1.6 . Along with the increasing TRIS content, the Dk value dropped slowly and reached the minimum value of 19.7 ± 1.1 .

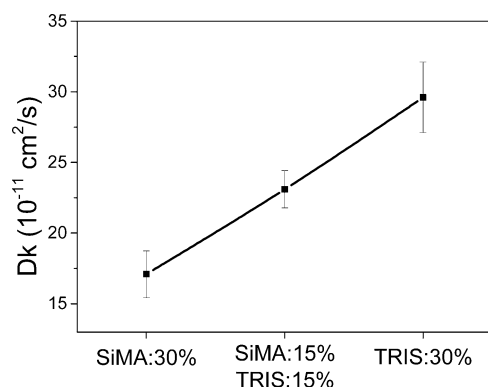
Table 3. Copolymerization Formulations for the Multicomponent Hydrogels with Different Types of Silicon-Containing Monomers, i.e., SiMA and TRIS

hydrogel	SiMA (wt %)	TRIS (wt %)	HEMA (wt %)	NVP (wt %)	DMA (wt %)	Dk (10^{-11} cm ² /s)	EWC (wt %)
III	30 \pm 0.1	0	38.5 \pm 0.1	16.5 \pm 0.1	15.0 \pm 0.1	17.8 \pm 1.2	40.1 \pm 1.6
IX	15 \pm 0.1	15 \pm 0.1	38.5 \pm 0.1	16.5 \pm 0.1	15.0 \pm 0.1	23.1 \pm 1.3	34.3 \pm 1.5
X	0	30 \pm 0.1	38.5 \pm 0.1	16.5 \pm 0.1	15.0 \pm 0.1	29.6 \pm 2.5	30.6 \pm 1.2

at a TRIS content of 10 wt %. After that, the Dk value began to rise with the increase of TRIS content and reached 29.6 ± 2.5 at a TRIS content of 30 wt %. Figure S2B (Supporting Information) shows the relationship between Dk and the percentage of EWC. As shown in Figure S2B (Supporting Information), the Dk value also did not always increase with the increase of EWC in hydrogels containing TRIS. The Dk value decreased from 29.6 ± 2.5 to 25.8 ± 2.3 when the percentage of EWC increased from 30.6 ± 1.2 to 43.5 ± 1.5 wt %. However, the Dk value began to increase when the EWC increased further. The Dk reached 32.1 ± 2.0 when the EWC was 64.0 wt %. Thus, the change rules of oxygen permeation as a function of both the contents of silicon monomer and the percentage of EWC in TRIS hydrogels are similar to those of SiMA hydrogels.

Therefore, as a summary, it is clear that the silicone–oxygen bond in the silicone phase and water in the hydrogel phase are two important channels for oxygen permeation. Because the silicon group and water cannot be reconciled together, a mutual inhibition competition mechanism exists between the silicone phase and the hydrogel phase. As a result of this mechanism, a minimum value of oxygen permeation always appeared. This mutual inhibition competition mechanism is rather universal for the hydrogel made of different silicon monomers, or at least it is suitable for both the SiMA and TRIS hydrogels presented in this paper.

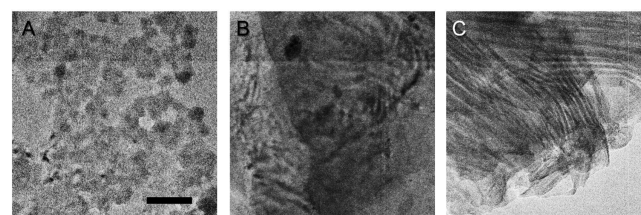
It is also important to know how different silicon containing monomers affect the oxygen permeation. Three different kinds of silicone hydrogels with the same weight percentage of silicon-containing monomers were prepared, and their formulations are shown in Table 3. The first hydrogel contained 30 wt % SiMA only, while the second one contained 15 wt % SiMA and 15 wt % TRIS and the third one contained 30 wt % TRIS only. Figure 4 shows the Dk values of these three silicone hydrogels. The Dk of these three silicone hydrogels were 17.8 ± 1.2 , 23.1 ± 1.3 , and 29.6 ± 2.5 , respectively. The

**Figure 4.** Value of Dk as a function of the ratio of SiMA and TRIS. The total percentage of SiMA and TRIS was maintained at 30 wt %, and the percentage of EWC was maintained at 35% for three silicone hydrogels.

Dk increased when SiMA was replaced by TRIS, which meant TRIS was a better material in terms of improving oxygen permeation.

One interesting finding is that the silicon content of the 30 wt % TRIS hydrogel is about 8% ($30\% \times 4 \times 28.1/422.8$), which is equal to the silicon content of 40 wt % SiMA hydrogel ($8\% = 40\% \times 3 \times 28.1/422.7$). However, the Dk of 30 wt % TRIS hydrogel (29.6 ± 2.5 in Figure 4) was much higher than that of 40 wt % SiMA hydrogel (19.3 ± 1.5 in Figure 1B). It means, in the silicone phase, the content of silicon–oxygen bonds is not the only factor that could affect the oxygen permeation. The internal morphology could also be an important factor in terms of the contribution to the oxygen permeation.

The internal morphologies of these three silicone hydrogels were also observed to explore the further relationship with oxygen permeability. Figure 5A is the TEM image of 30 wt %

**Figure 5.** TEM images showing the internal phase-separation structures of silicone hydrogels made from (A) 30 wt % SiMA, (B) 15 wt % SiMA and 15 wt % TRIS, and (C) 30 wt % TRIS. Scale bar = 200 nm.

SiMA hydrogel. The hydrogel showed a phase separation structure, whereas the silicone phase had a granular texture, which was similar to those shown in Figure 2. However, Figure 5C shows the internal morphology of 30 wt % TRIS hydrogel, which had a clearly different morphology. The silicone phase in TRIS hydrogel presented as a fibrous texture. The hydrogel made from half SiMA and half TRIS had the combined structure of both granular and fibrous texture, as shown in Figure 5B. It was clear that the fibrous texture of the silicone phase was more continuous than the granular texture, so it was easy to understand that the oxygen permeation of TRIS hydrogel was higher than that of SiMA hydrogel.

As we all know, the oxygen permeability of silicone hydrogels is affected by hydrogel domains and silicone domains. For the oxygen permeability mechanism of hydrogel domains, water content is a key factor. Water has at least three different states in hydrogel:⁴¹ (1) “hydration water” which combines with the hydrophilic groups on the polymer chain; (2) “intermediate water” which has weak interaction with hydrogel near the hydrophilic orientation; (3) “free water” which has the same properties as natural water and can freely diffuse in hydrogel. Oxygen permeation through aqueous domains mainly depends on “free water” in hydrogel.⁴²

About the oxygen permeability mechanism of silicone domains, silicone polymers are well-known for their high oxygen permeability compared with that of conventional hydrogels. High gas permeability is associated with polymers with spherical substituents, while the gas permeability is not significantly enhanced by long alkyl pendant groups. The bulkiness of the siloxane group and chain mobility characterizes the high oxygen permeability of silicone materials.⁴³ The high oxygen permeability of silicone polymers presumably derives from their low cohesive energy structure, stiff main chain, and bulky substituents.⁴⁴ Thus, the oxygen permeability of silicone domains depends on the amount of siloxane keys in the silicon monomers and the proportion of silicon monomers in the material.

Therefore, in silicone hydrogel, it is important and significant to figure out how these two different domains work together to contribute to the oxygen permeability. Because these two factors cannot be reconciled together, they can work as either a competitive rule or a synergy relationship or even a more complex relationship. Our results showed that a universal mutual inhibition competition exists between the silicone phase and the hydrogel phase. As a result of this mechanism, a minimum value of oxygen permeation always appeared. A similar rule had been found in previous research. Lai et al. have reported on the relationship between oxygen permeability and EWC and that between oxygen permeability and silicon atom content in hydrogels derived from prepolymer IDS3H and DMA.³⁵ Kunzler et al. have reported on the oxygen permeability of a range of silicone hydrogel materials based on tris(trimethylsiloxy)silyl propyl vinylcarbamate (TPVC) and *N*-vinylpyrrolidinone (NVP).⁴⁵ Willis et al. have done some research based on Kunzler's work and indicated we can tailor the oxygen permeability characteristics of hydrogels by controlling the silicone:hydrophilic monomer balance.¹² Pozuelo et al. have also found this similar rule and structured Si-Hy matrices to explain the oxygen permeability–water content relationship. They presented a hypothesis that the hydrophilic and hydrophobic phases are separately formed but they coexist and there is a continuous link between them.³⁹

The purpose of the above research was to improve the oxygen permeability of hydrogels, so the long-chain branched silicone prepolymers were chosen. A phenomenon would appear that the oxygen permeability of the silicone phase was much stronger than that of the hydrogel phase. It would lead to a highly unbalanced relationship. The competitive relation was not obvious because the hydrogel phase was at a more disadvantaged position. Sun et al. have utilized a molecular simulation study to discuss the effect of water content and silicon monomer content on oxygen permeation in PSiMA–IPN–PMPC hydrogel. They have calculated the diffusion coefficients for water in different domains at varying water contents from 10 to 30 wt %.⁴⁶

We have prepared silicone hydrogels containing SiMA contents varying from 10 to 50 wt %. The oxygen permeability–water content relationship and the oxygen permeability–silicon monomer content relationship we had found were similar to them in previous research. However, the competitive relationship was more obvious in our work. We analyzed the effect of internal micromorphology on the oxygen permeability of multicomponent copolymerized hydrogel by observing the microphase separation structure in hydrogels by TEM.

Furthermore, the most important finding of our work is that the oxygen transmission also depended on the morphology of the silicone phase. The fibrous texture of the silicone phase is a better structure for oxygen permeation than granular structure.

In summary, the oxygen permeation mechanism of silicone hydrogel depended on three factors, the percentage of water in the hydrogel phase, the content of the silicon–oxygen bond in the silicone phase, and the internal morphology of the silicone phase. The first two factors work by a mutual inhibition competition way. Furthermore, the morphology of the silicone phase is also an important factor that affects the oxygen transmission. These results will help us to design silicone hydrogels with better properties and wider application in contact lenses.

CONCLUSIONS

In this Article, the multicomponent copolymers were prepared by the copolymerization of two silicon-containing monomers SiMA and TRIS with three hydrophilic monomers HEMA, NVP, and DMA. The EWC, Dk, and internal morphologies of the obtained hydrogels were measured, and their relationships were discussed in detail. The results show that the EWC decreased with the increase of SiMA content. The relationship between Dk and the silicon monomer content as well as the relationship between Dk and EWC showed an inverted bell curve distribution, which means the silicon–oxygen bond in silicone and water in hydrogel follows a mutual inhibition competition rule. Besides, TEM results show that the morphology of the silicone phase plays an important role in oxygen permeation. The fibrous texture of the silicone phase in TRIS hydrogel results in a bigger Dk value than the granular texture in SiMA hydrogel.

ASSOCIATED CONTENT

Supporting Information

Figure S1 and Table S1 show the cross-section images observed by SEM (Figure S1) and the weight percentage of elements analyzed by EDS (Table S1) of the silicone hydrogels with different percentages of SiMA. Tables S2 and S3 present the copolymerization formulations for multicomponent hydrogels with different contents of TRIS monomer (Table S2) and MAA monomer (Table S3). Figure S2 shows the value of the oxygen permeability coefficient (Dk) as a function of the TRIS percentage (Figure S2A) and as a function of the percentage of EWC (Figure S2B) in the silicone hydrogels. This material is available free of charge via the Internet at <http://pubs.acs.org>.

AUTHOR INFORMATION

Corresponding Author

*Phone: +86 139 139 931 09. E-mail: yj@seu.edu.cn. Web: <http://jianglab.net>.

Notes

The authors declare no competing financial interest.

ACKNOWLEDGMENTS

This work was supported by the National Natural Science Foundation of China (NSFC) with grant number 21174029 and the Industry Academia Cooperation Innovation Fund of Jiangsu Province with grant number BY2014127-07 to Y.J.

REFERENCES

- (1) Ragauskas, A. J.; Williams, C. K.; Davison, B. H.; Britovsek, G.; Cairney, J.; Eckert, C. A.; Frederick, W. J.; Hallett, J. P.; Leak, D. J.; Liotta, C. L.; et al. The Path forward for Biofuels and Biomaterials. *Science* **2006**, *311*, 484–489.
- (2) Augst, A. D.; Kong, H. J.; Mooney, D. J. Alginate Hydrogels as Biomaterials. *Macromol. Biosci.* **2006**, *6*, 623–633.
- (3) Mikos, A. G.; Sarakinos, G.; Leite, S. M.; Vacanti, J. P.; Langer, R. Laminated 3-Dimensional Biodegradable Foams for Use in Tissue Engineering. *Biomaterials* **1993**, *14*, 323–330.
- (4) Shoichet, M. S. Polymer Scaffolds for Biomaterials Applications. *Macromolecules* **2010**, *43*, 581–591.
- (5) Debord, J. D.; Lyon, L. A. Thermoresponsive photonic crystals. *J. Phys. Chem. B* **2000**, *104*, 6327–6331.
- (6) Kodjikian, L.; Burillon, C.; Roques, C.; Pellon, G.; Frenay, J.; Renaud, F. N. R. Bacterial Adherence of *Staphylococcus Epidermidis* to Intraocular Lenses: A Bioluminescence and Scanning Electron Microscopy Study. *Invest. Ophthalmol. Visual Sci.* **2003**, *44*, 4388–4394.
- (7) Seal, B. L.; Otero, T. C.; Panitch, A. Polymeric Biomaterials for Tissue and Organ Regeneration. *Mater. Sci. Eng., R* **2001**, *34*, 147–230.
- (8) Naskar, J.; Palui, G.; Banerjee, A. Tetrapeptide-Based Hydrogels: for Encapsulation and Slow Release of an Anticancer Drug at Physiological pH. *J. Phys. Chem. B* **2009**, *113*, 11787–11792.
- (9) Hench, L. L. Bioceramics - From Concept to Clinic. *J. Am. Ceram. Soc.* **1991**, *74*, 1487–1510.
- (10) Suchanek, W.; Yoshimura, M. Processing and Properties of Hydroxyapatite-Based Biomaterials for Use as Hard Tissue Replacement Implants. *J. Mater. Res.* **1998**, *13*, 94–117.
- (11) Suh, J. K. F.; Matthew, H. W. T. Application of Chitosan-Based Polysaccharide Biomaterials in Cartilage Tissue Engineering: A Review. *Biomaterials* **2000**, *21*, 2589–2598.
- (12) Willis, S. L.; Court, J. L.; Redman, R. P.; Wang, J. H.; Leppard, S. W.; O'Byrne, V. J.; Small, S. A.; Lewis, A. L.; Jones, S. A.; Stratford, P. W. A Novel Phosphorylcholine-Coated Contact Lens for Extended Wear Use. *Biomaterials* **2001**, *22*, 3261–3272.
- (13) Barrie, J. A.; Munday, K. Gas-transport in Heterogeneous Polymer Blends.1. Polydimethylsiloxane-G-Polystyrene and Polydimethylsiloxane-B-Polystyrene. *J. Membr. Sci.* **1983**, *13*, 175–195.
- (14) Barrie, J. A.; Williams, M. J. L.; Spencer, H. G. Gas-transport in Heterogeneous Polymer Blends.3. Alternating Block Copolymers of Poly(Bisphenol-A Carbonate) and Polydimethylsiloxane. *J. Membr. Sci.* **1984**, *21*, 185–202.
- (15) Barrie, J. A.; Sagoo, P.; Thomas, A. G. Gas-transport in Heterogeneous Polymer Blends.4. Natural Rubber-G-Polystyrene. *J. Membr. Sci.* **1989**, *43*, 229–242.
- (16) Barnabeo, A. E.; Creasy, W. S.; Robeson, L. M. Gas Permeability Characteristics of Nitrile-Containing Block and Random Copolymers. *J. Polym. Sci., Polym. Chem.* **1975**, *13*, 1979–1986.
- (17) Fujimoto, T.; Ohkoshi, K.; Miyaki, Y.; Nagasawa, M. Artificial Membranes from Multiblock Copolymers.1. Fabrication of a Charge-Mosaic Membrane and Preliminary Tests of Dialysis and Piezodialysis. *J. Membr. Sci.* **1984**, *20*, 313–324.
- (18) Chiou, J. S.; Paul, D. R. Gas Permeation in Miscible Blends of Poly(Methyl Methacrylate) with Bisphenol Chloral Polycarbonate. *J. Appl. Polym. Sci.* **1987**, *33*, 2935–2953.
- (19) Lee, Y. K.; Tak, T. M.; Lee, D. S.; Kim, S. C. Cationic Anionic Interpenetrating Polymer Network Membranes for the Pervaporation of Ethanol Water Mixture. *J. Membr. Sci.* **1990**, *52*, 157–172.
- (20) Lee, D. S.; Jung, D. S.; Kim, T. H.; Kim, S. C. Gas-transport in Polyurethane Polystyrene Interpenetrating Polymer Network Membranes.1. Effect of Synthesis Temperature and Molecular-Structure Variation. *J. Membr. Sci.* **1991**, *60*, 233–252.
- (21) Lee, D. S.; Kang, W. K.; An, J. H.; Kim, S. C. Gas-transport in Polyurethane Polystyrene Interpenetrating Polymer Network Membranes.2. Effect of Cross-linked State and Annealing. *J. Membr. Sci.* **1992**, *75*, 15–27.
- (22) Tsujita, Y.; Yoshimura, K.; Yoshimizu, H.; Takizawa, A.; Kinoshita, T.; Furukawa, M.; Yamada, Y.; Wada, K. Structure and Gas-Permeability of Siloxane Imide Block-Copolymer Membranes.1. Effect of Siloxane Content. *Polymer* **1993**, *34*, 2597–2601.
- (23) Ban, S.; Huang, C.; Yuan, X. Z.; Wang, H. J. Molecular Simulation of Gas Adsorption, Diffusion, and Permeation in Hydrated Nafion Membranes. *J. Phys. Chem. B* **2011**, *115*, 11352–11358.
- (24) Liu, Q. L.; Huang, Y. Transport Behavior of Oxygen and Nitrogen through Organasilicon-Containing Polystyrenes by Molecular Simulation. *J. Phys. Chem. B* **2006**, *110*, 17375–17382.
- (25) Clayden, N. J.; Nijs, C.; Eeckhaut, G. Study of the Polymer Morphology in Urethane Elastomers by Solid State H-2 NMR and Small Angle X-ray Scattering. *Macromolecules* **1998**, *31*, 7820–7828.
- (26) Garrett, J. T.; Runt, J.; Lin, J. S. Microphase Separation of Segmented Poly(Urethane Urea) Block Copolymers. *Macromolecules* **2000**, *33*, 6353–6359.
- (27) Koberstein, J. T.; Russell, T. P. Simultaneous SAXS-DSC Study of Multiple Endothermic Behavior in Polyether-based Polyurethane Block Copolymers. *Macromolecules* **1986**, *19*, 714–720.
- (28) Ryan, A. J.; Macosko, C. W.; Bras, W. Order-disorder Transition in a Block Copolyurethane. *Macromolecules* **1992**, *25*, 6277–6283.
- (29) Velankar, S.; Cooper, S. L. Microphase Separation and Rheological Properties of Polyurethane Melts. 2. Effect of Block Incompatibility on the Microstructure. *Macromolecules* **2000**, *33*, 382–394.
- (30) Metters, A. T.; Bowman, C. N.; Anseth, K. S. A Statistical Kinetic Model for the Bulk Degradation of PLA-b-PEG-b-PLA Hydrogel Networks. *J. Phys. Chem. B* **2000**, *104*, 7043–7049.
- (31) Nicolson, P. C. Continuous Wear Contact Lens Surface Chemistry and Wearability. *Eye Contact Lens* **2003**, *29*, S30–2 discussion S57–9, S192–4..
- (32) Friends, G. D.; Kunzler, J. F.; Ozark, R. M. Recent Advances in the Design of Polymers for Contact-lenses. *Macromol. Symp.* **1995**, *98*, 619–631.
- (33) Chekina, N. A.; Pavlyuchenko, V. N.; Danilichev, V. F.; Ushakov, N. A.; Novikov, S. A.; Ivanchev, S. S. A New Polymeric Silicone Hydrogel for Medical Applications: Synthesis and Properties. *Polym. Adv. Technol.* **2006**, *17*, 872–877.
- (34) Chaouk, H.; Wilkie, J. S.; Meijs, G. F.; Cheng, H. Y. New Porous Perfluoropolyether Membranes. *J. Appl. Polym. Sci.* **2001**, *80*, 1756–1763.
- (35) Lai, Y. C. Novel Polyurethane Silicone Hydrogels. *J. Appl. Polym. Sci.* **1995**, *56*, 301–310.
- (36) Liu, L.; Sheardown, H. Glucose Permeable Poly(dimethyl siloxane) Poly(N-isopropyl acrylamide) Interpenetrating Networks as Ophthalmic Biomaterials. *Biomaterials* **2005**, *26*, 233–244.
- (37) Maldonado-Codina, C.; Morgan, P. B.; Schnider, C. M.; Efron, N. Short-term Physiologic Response in Neophyte Subjects Fitted with Hydrogel and Silicone Hydrogel Contact Lenses. *Optom. Visual Sci.* **2004**, *81*, 911–921.
- (38) Wang, J. J.; Li, X. S. Improved Oxygen Permeability and Mechanical Strength of Silicone Hydrogels with Interpenetrating Network Structure. *Chin. J. Polym. Sci.* **2010**, *28*, 849–857.
- (39) Pozuelo, J.; Compan, V.; Gonzalez-Mejome, J. M.; Gonzalez, M.; Molla, S. Oxygen and Ionic Transport in Hydrogel and Silicone-Hydrogel Contact Lens Materials: An Experimental and Theoretical Study. *J. Membr. Sci.* **2014**, *452*, 62–72.
- (40) Zhao, Z. B.; An, S. S.; Xie, H. J.; Jiang, Y. The Copolymerization and Properties of Multicomponent Crosslinked Hydrogel. *Chin. J. Polym. Sci.* **2015**, *33*, 173–183.
- (41) Wang, J. H.; Fonn, D.; Simpson, T. L.; Sorbara, L.; Kort, R.; Jones, L. Topographical Thickness of the Epithelium and Total Cornea after Overnight Wear of Reverse-Geometry Rigid Contact Lenses for Myopia Reduction. *Invest. Ophthalmol. Visual Sci.* **2003**, *44*, 4742–4746.
- (42) Refojo, M. F.; Leong, F. L. Water-dissolved-Oxygen Permeability Coefficients of Hydrogel Contact-lensed and Boundary-Layer Effects. *J. Membr. Sci.* **1979**, *4*, 415–426.
- (43) Goda, T.; Ishihara, K. Soft Contact Lens Biomaterials from Bioinspired Phospholipid Polymers. *Expert Rev. Med. Devices* **2006**, *3*, 167–174.

(44) Nagai, K.; Masuda, T.; Nakagawa, T.; Freeman, B. D.; Pinnau, I. Poly 1-(trimethylsilyl)-1-propyne and Related Polymers: Synthesis, Properties and Functions. *Prog. Polym. Sci.* **2001**, *26*, 721–798.

(45) Kunzler, J. F. Silicone Hydrogels for Contact Lens Application. *Trends Polym. Sci.* **1996**, *4*, 52–59.

(46) Sun, D. L.; Zhou, J. Effect of Water Content on Microstructures and Oxygen Permeation in PSiMA-IPN-PMPC Hydrogel: A Molecular Simulation Study. *Chem. Eng. Sci.* **2012**, *78*, 236–245.